Available online at www.sciencedirect.com
SCIENCE DIRECT®
Journal of Nuclear Materials 337–339 (2005) 802–807
journal of nuclear materials
www.elsevier.com/locate/jnucmat

Study of plasma wall interactions in the long-pulse NB-heated discharges of JT-60U towards steady-state operation

H. Takenaga *, N. Asakura, S. Higashijima, T. Nakano, H. Kubo, S. Konoshima, N. Oyama, A. Isayama, S. Ide, T. Fujita, Y. Miura, The JT-60 team

Department of Fusion Plasma Research, Naka Fusion Research Establishment, Japan Atomic Energy Research Institute, Naka-machi, Naka-gun, Ibaraki-ken 311-0193, Japan

Abstract

Long time scale variation of plasma-wall interactions and its impact on particle balance, main plasma performance and particle behavior have been investigated in ELMy H-mode plasmas by extending the discharge pulse and the neutral beam heating pulse to 65 s and 30 s, respectively. The wall pumping rate starts to decrease in the latter phase by repeating the long-pulse discharges with 60% of Greenwald density sustained by gas-puffing. After several discharges, the wall inventory is saturated in the latter phase and, consequently, the density increases with neutral beam fuelling only. The edge pressure in the main plasma is reduced and ELMs are close to the type III regime under conditions of wall saturation. The intensities of C II emission near the X-point and CD band emission in the inner divertor start to increase before the wall saturates and continue to increase after the wall is saturated.

PACS: 52.25.−b; 52.25.Vy; 52.25.Ya; 52.40.Hf; 52.55.Fa
Keywords: Density control; Divertor plasma; JT60U; Particle balance; Wall pumping

1. Introduction

In JT-60U, high performance plasmas have been developed to provide a physics basis for ITER [1] and advanced steady-state tokamak reactors such as SSTR [2]. The equivalent break-even condition (equivalent DT fusion gain of 1.25) has been demonstrated in the reversed magnetic shear configuration with an internal transport barrier [3]. For realizing a steady-state operation in a fusion reactor, it is also important to extend the duration of these high performance plasmas. For this goal, sustainment of high performance plasmas longer than a time scale of the variation of plasma-wall interactions is one of the key issues. In a short pulse discharge, the particle absorption at the wall (wall pumping) largely contributes to the density control. High confinement plasmas have been achieved by avoiding confinement degradation at high density using the wall pumping. However, the wall pumping is expected to be less effective in the long-pulse discharge due to the

* Corresponding author.
E-mail address: takenaga@naka.jaeri.go.jp (H. Takenaga).

0022-3115/$ - see front matter
doi:10.1016/j.jnucmat.2004.10.096

saturation of the wall inventory (wall saturation). It is important to understand the time scale of the wall saturation and to develop the particle control during the wall saturation.

In JT-60U, the discharge pulse length has been recently extended from 15 s to 65 s together with the extension of the NB heating pulse length from 10 s to 30 s, since no wall saturation was observed during 15 s discharges [4]. In the long-pulse discharge, the increase in the time-integrated particle flux to the divertor plates and the higher plate temperature resulting from the larger energy input enhances the rate of wall saturation. This is because the wall inventory decreases with increasing wall temperature in the range of >150–200 °C [5]. On the other hand, co-deposition with carbon impurity slows the wall saturation rate, because carbon impurity deposition to the wall surface generates a new fresh surface. In long-pulse discharges of TRIAM-1M, wall saturation and wall pumping were repeated with a time scale of several tens of minutes, and the discharge duration of high density plasmas ($>2.5\times10^{19}\,m^{-3}$) were limited to about 10 s due to the wall saturation [6]. After installation of the cooling system, in long-pulse discharges of Tore Supra, wall saturation was not observed for more than 4 min [7], although the density was increased before the installation [8]. In divertor plasmas of JET, the density increased in the latter phase of a 1 min discharge [9]. In this paper, the time scale and the key parameters of the wall saturation, and impacts of the wall saturation on particle balance, pedestal and ELM characteristics and particle behavior of deuterium and carbon impurity are investigated. It is noted that the wall pumping includes the particle absorption at both divertor plates and first wall, and in this paper, the term 'wall saturation' means that the net wall pumping rate is equal to zero.

In Section 2, the modifications for the long-pulse discharge and initial results are briefly described. In Section 3, the particle balance is quantitatively analyzed in the long-pulse discharges. The main plasma performance and the particle behavior of deuterium and carbon impurities under the wall saturation are investigated in Section 4, followed by a summary in Section 5.

2. Extension of discharge and heating pulse length

In JT-60U, the W-shaped divertor formed by the inner and outer inclined divertor plates and the dome in the private flux region was installed with the divertor pumping from both inner and outer private flux regions. The divertor pumping rate can be controlled with shutters during the discharge. CFC tiles are used for the divertor plates, the dome top and the outer dome wing, and graphite tiles are used for the inner dome wing, the baffle plates and the first wall around the main plasma. Previously the discharge duration was limited to 15 s with a plasma current (I_p) of 3 MA and a toroidal magnetic field (B_T) of 4 T. Recently, the discharge duration has been extended up to 65 s with $I_p \sim 1$ MA and $B_T = 2.7$ T. The NB heating duration has also been extended from 10 s with the heating power (P_{NB}) of ~30 MW to 30 s with $P_{NB} = 14$ MW.

The long-pulse experiments were performed in the 2003 JT-60U experiment campaign where the vacuum vessel was baked at 150 °C. A 65 s tokamak discharge of $I_p = 0.7$ MA and 59.8 s flat top with divertor configuration was obtained with NB pulse length fully extended to 30 s of the positive-ion source based NB (P-NB). The total input energy of 350 MJ, including the negative-ion source based NB (N-NB) and ECRF powers (which will increase since the systems are being conditioned at this time), has been achieved with 10–14 MW heating power. No sudden increase of carbon generation such as a carbon bloom was observed even with this energy input in the W-shaped divertor. This contrasts with previous results from the JT-60U open divertor, where the sudden increase of the carbon generation was observed with 70 MJ input [10]. ELMy H-mode plasmas were successfully sustained for about 30 s, and a value of normalized beta (β_N) of 1.9, which is comparable to the ITER standard operation, is sustained for ~24 s with an ITER relevant safety factor at the 95% flux surface ($q_{95} \sim 3.2$). In the latter phase of this discharge, the current profile reached a steady-state. Strong MHD activity such as the neoclassical tearing mode was not observed during the discharge. However, Dα emission intensity between ELMs and the electron density increased, and energy confinement enhancement factor (H_{89PL}) decreased from 1.9 to 1.7. This indicates that the plasma-wall interaction is a critical issue for sustainment of high confinement.

3. Particle balance in long-pulse ELMy H-mode discharges

3.1. Relation between wall pumping and wall temperature

The particle balance is quantitatively analyzed in long-pulse ELMy H-mode plasmas. The ELMy H-mode plasmas are successfully sustained for about 30 s at $I_p = 1.0$ MA and $B_T = 2.1$ T with $P_{NB} = 12$–14 MW as shown in Fig. 1. In this discharge, feedback control of the line averaged electron density ($\bar{n}_e$) using the gas-puffing was applied to keep a constant density of about $2.8\times10^{19}\,m^{-3}$, which corresponds to 60% of the Greenwald density (n_{GW}). However, the value of $\bar{n}_e$ is smaller than the target density even with large gas-puffing rate before $t = 25$ s. After $t = 25$ s, $\bar{n}_e$ gradually increases and the gas-puffing rate decreases, indicating reduction in the wall pumping rate. The divertor pumping rate can be estimated from the reduction in the gas-puffing

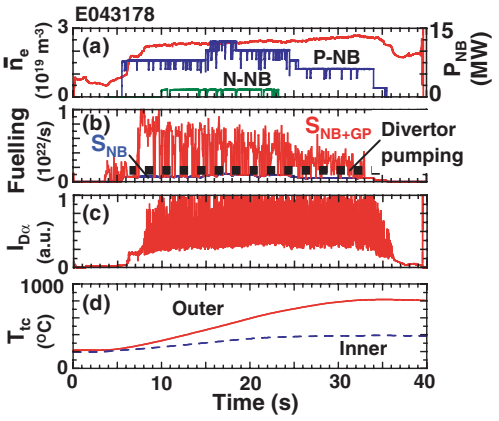

Fig. 1. Typical waveforms of the long-pulse ELMy H-mode plasma. (a) Line averaged electron density and heating power of positive and negative-ion source based NB (P-NB and N-NB). (b) NB fuelling rate (S_{NB}) and total (NB + Gas-puffing) fuelling rate (S_{NB+GP}). The dashed line indicates the divertor pumping rate. FB control is stopped at $t = 33$ s. (c) Dα emission intensity from the outer divertor. (d) Divertor plate temperature measured at ~5 mm below the surface around the outer strike point (solid line) and the inner strike point (dashed line).

rate necessary for keeping a constant density by closing the divertor pumping shutter [4]. The divertor pumping rate is estimated to be $1.8 \times 10^{21}\,s^{-1}$ in similar discharges. In this discharge, the wall pumping rate is estimated to be $3.1 \times 10^{21}\,s^{-1}$ at $t = 10.5$ s and $8 \times 10^{21}\,s^{-1}$ at $t = 30.5$ s, respectively. The wall pumping rate is roughly estimated to be 5.5% ($t = 10.5$ s) and 1.2% ($t = 30.5$ s) of the recycling flux, respectively. Although the wall pumping rate decreases to a level smaller than the divertor pumping in the latter phase, the wall is not saturated.

The divertor plate temperature measured with a thermocouple ~5 mm below the surface (T_{tc}) reaches 800 °C around the outer strike point and 400 °C around the inner strike points, respectively. Using a heat transfer calculation, the surface temperature is estimated to be higher by 100–200 °C than T_{tc}. The surface temperature around both strike points is sufficiently higher than a critical temperature for the region where wall inventory decreases with increasing surface temperature [5]. In this region, the wall retention is reduced by a factor of more than 3 compared with the region of 150 °C. In this discharge, the number of the total injected particles reaches to about 1.1×10^{23} particles and the wall inventory is estimated to be about 6×10^{22} particles. When it is assumed that 6×10^{22} particles are absorbed in a toroidal band 20 cm in width (~particle flux width) with D/C = 0.4, the thickness of the layer is calculated to be ~0.36 μm. This thickness cannot be explained without co-deposition. Co-deposition might be responsible for the fact that the wall saturation is not observed even with high plate temperature around the strike points. However, the JT-60U tile analysis indicates that D/C ratio is much smaller than 0.4 [11]. Therefore, wider absorption area with the low temperature around the high temperature area might contribute to the wall pumping.

3.2. Effects of discharge history on the wall pumping

In order to investigate effects of discharge history on the wall pumping, the long-pulse discharges similar to the discharge shown in Fig. 1 are repeated. In the early discharges (see Fig. 2(a): E042716), the almost constant gas-puffing rate of $2.5–3.5 \times 10^{21}\,s^{-1}$ is necessary for keeping a constant density for about 30 s. The wall

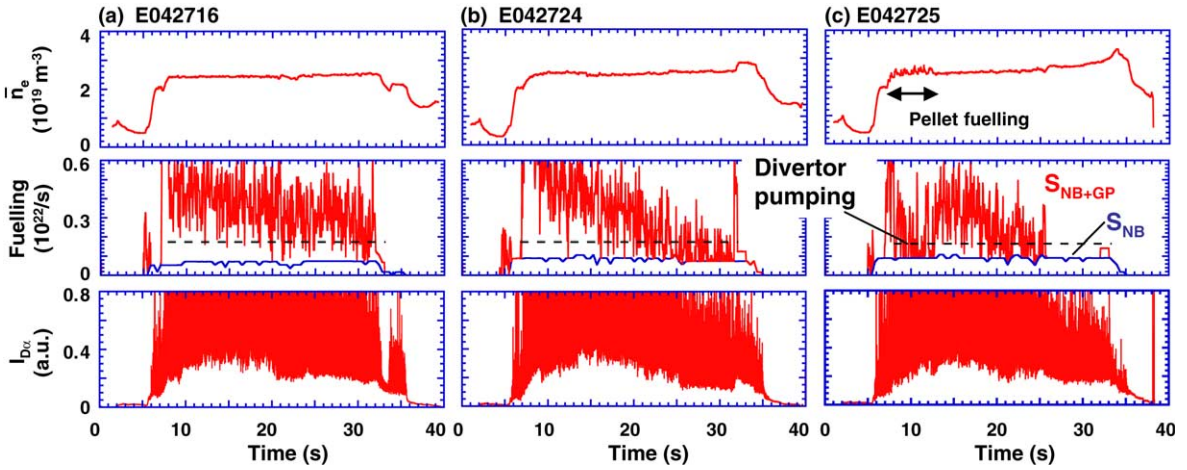

Fig. 2. History of the long-pulse ELMy H-mode plasma in a day: line averaged electron density, fuelling rate and Dα emission intensity from the inner divertor. The dashed line in the second column indicates the divertor pumping rate.

pumping rate is estimated to be $2.6\times10^{21}\,s^{-1}$ at $t = 10.5$ s and $1.4\times10^{21}\,s^{-1}$ at $t = 28.5$ s. The wall pumping rate is similar to the divertor pumping rate even in the latter phase ($t > 25$ s). In this discharge, the number of the total injected particles reaches to about 1×10^{23} particles.

After several long-pulse discharges as shown in Fig. 2(b) (E042724), the gas-puffing rate for keeping the density constant starts to decrease during the discharge and it reduces by a factor of 3 in the latter phase. At the same time, the total fuelling rate decreases to the same level as the divertor pumping rate, indicating that the wall is nearly saturated in the latter phase. However, $\bar{n}_e$ is controlled to be almost constant with the nearly saturated wall. The number of the total injected particles is estimated to be 8.6×10^{22}, which is smaller than that of E042716 (Fig. 2(a)). The wall condition such as initial wall inventory before the discharge is important for the wall saturation.

The effects of the wall condition are clearly observed in the next discharge as shown in Fig. 2(c) (E042725). In this discharge, pellets are injected from the high-field-side during $t = 7$–13 s. In this period, the gas-puffing rate is reduced. The density starts to increase without gas-puffing and reaches to 77% of n_{GW} with occurrence of X-point MARFE in the final phase of the NB heating. The wall pumping rates are estimated to be $2.8\times10^{21}\,s^{-1}$ in the early phase ($t = 10$ s). In the latter phase, the total fuelling rate is smaller than the divertor pumping rate. The density is uncontrollable in the latter phase even with the divertor pumping, however, a disruption does not occur. The number of total injected particles is 6.8×10^{22} including the particles injected as the pellets. These phenomena are observed for the first time after the extension of the NB heating pulse length and are ascribed to the change of wall conditions with the long time scale.

The wall inventory is estimated to be about 4–5×10^{22} particles in the early discharges, decreasing to 2–3×10^{22} particles after the 3rd discharge, in which divertor pumping is off. This is the case even though He TDC was performed between shots. In the discharges after an OH discharge or no build-up shot (break-down only), the wall inventory recovers to 4×10^{22} particles. However, in the next discharges, the wall inventory is reduced to 2×10^{22} particles. In this discharge series, the wall temperature was not measured. However, the increase of the offset wall temperature in this discharge series is estimated to be less than 50–70 °C based on the data in another discharge series. This suggests that the increase in the offset wall temperature is not important for the wall saturation, because the offset wall temperature is not sufficiently higher than the critical temperature at which the wall inventory decreases with increasing surface temperature. The significant effects of the discharge history on the wall pumping also support the observations that the absorption area with the low temperature is dominant for wall pumping rather than the co-deposition.

4. Impacts of wall saturation on plasma properties

In this section, H-mode pedestal and ELM characteristics and particle behavior of deuterium and carbon impurity are discussed for understanding the impacts of the wall saturation on both the main and divertor plasmas. The discharge shown in Fig. 2(c), where the wall saturation was observed in the latter phase, is investigated.

4.1. H-mode pedestal and ELMs

The value of H_{89PL} decreases from 1.5 at $n_e/n_{GW} = 0.6$ in the early phase ($t = 9.8$ s) to 1.3 at $n_e/n_{GW} = 0.7$ in the latter phase ($t = 31.4$ s). This confinement degradation seems to be consistent with the degradation at high densities. The n–T diagram at $r/a = 0.85$ near the pedestal top is shown in Fig. 3. The edge pressure decreases in the latter phase ($t > 25$ s), where $\bar{n}_e$ increases without gas-puffing. The temperature tends to decrease before the increase in density. Fig. 4 shows the time evolution of Dα emission intensity in the outer divertor. In the early phase of the discharge ($t = 10$ s), Type I ELMs are observed with a frequency of ~150 Hz. In the middle phase ($t = 20$ s), the base intensity of Dα emission slightly increases, and Type III ELMs start to appear between Type I ELMs (mixture ELM). The frequency of Type I ELMs is evaluated to be ~120 Hz, which slightly decreases. In the latter phase of the discharge ($t = 33$ s), the base intensity of Dα

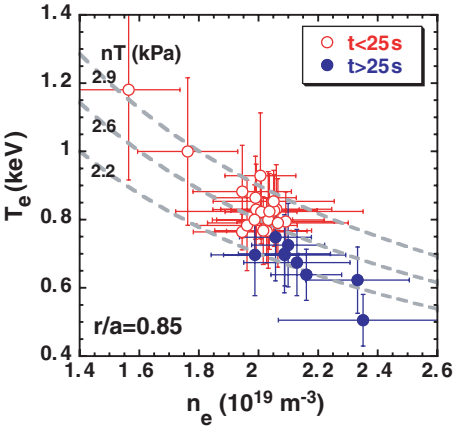

Fig. 3. n–T diagram at $r/a = 0.85$ in the discharge (E042725) where the wall saturation is observed. Open and closed circles show the data before and after $t = 25$ s, respectively. Dashed lines show the curves with pressures of 2.2, 2.6 and 2.9 kPa.

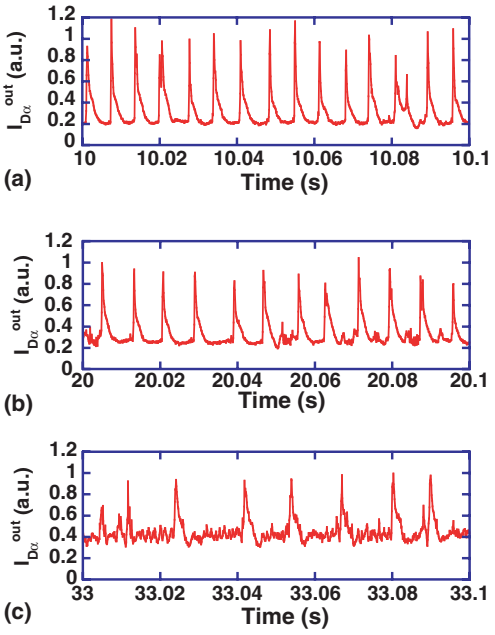

Fig. 4. Dα emission intensity from the outer divertor in (a) early phase (t = 10–10.1 s), (b) middle phase (t = 20–20.1 s) and (c) latter phase (t = 33–33.1 s) in the discharge of E042725.

emission is larger by a factor of 2 than that in the early phase. The ELMs are close to Type III regime, although Type I like ELMs are observed. The frequency of the Type I like ELMs is smaller than the Type I ELM frequencies in the early and middle phase. These characteristics of the H-mode pedestal and ELMs are similar to that in the short pulse discharge at high density.

4.2. Neutral particle behavior

When the absorption area at the low wall temperature is important for the wall pumping, the poloidal distribution of the Dα emission intensity might be changed during the wall saturation. Fig. 5 shows the poloidal distribution of the Dα emission intensity at t = 10 s (no wall saturation), t = 25 s (density starts to increase without gas-puffing) and t = 33 s (wall saturation). The emission is averaged over 100 ms, thus, the emission during the ELM is included. The poloidal distribution of the Dα emission intensity at t = 25 s (pluses) is almost the same as that at t = 10 s (circles) except in outer divertor. An increase in Dα emission intensity is not observed around the main plasma and in the inner divertor. The Dα emission intensity increases at channel number 10. The increase in the Dα emission intensity in the upstream of the outer divertor is usually observed with an X-point MARFE even in the 15 s discharge. Two reasons can be considered, i.e. particle release at the outer dome wing due to the wall saturation and deeper penetration

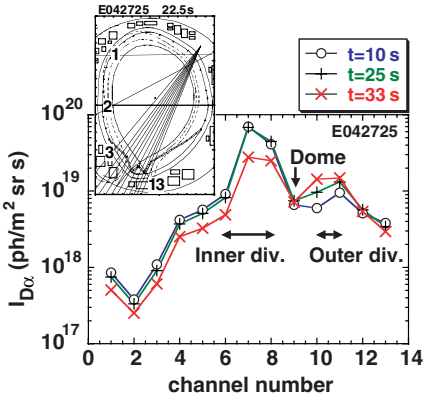

Fig. 5. Poloidal distribution of Dα emission intensity in the discharge of E042725. Circles, pluses and crosses show the data at t = 10 s, 25 s and 33 s, respectively. The sight lines are shown in the inset.

of the neutral particles recycled around outer strike point. At present, no definitive answer has yet emerged, and further work is to be done. At t = 33 s with the X-point MARFE, the Dα emission intensity in the region around the main plasma and the inner divertor decreases and the in-out asymmetry becomes weak as shown by crosses. In the outer divertor, the Dα emission intensity becomes large in the upstream of the divertor plasma (channel number 10). These changes of the Dα emission intensity profile are similar to the changes observed in the 15 s discharge with the X-point MARFE under the conditions of non-saturated wall pumping.

4.3. Carbon impurity behavior

Fig. 6 shows the time evolution of (a) the C II emission intensities around the inner and outer strike points and the X-point and (b) the CD band emission intensity from the inner divertor. The C II emission intensity near the X-point increases from t = 17 s before the wall saturation, while the emissions from the inner and outer divertor regions are almost constant. Consequently, the C II emission intensity profile has a peak near the X-point during the X-point MARFE. This increase in C II emission intensity near the X-point is also observed even without wall saturation case, although the increase in the emission is smaller and has no peak near the X-point. Therefore, the increase in C II emission near the X-point is not directly caused by the wall saturation. The time behavior of the CD band emission intensity is similar to the behavior of the C II emission intensity near the X-point. It suggests that the increase in the C II emission intensity is related to chemical sputtering. In these discharges, the temperature of the divertor plates was not measured. However, in the similar discharges shown in Fig. 1, the divertor plates temperature

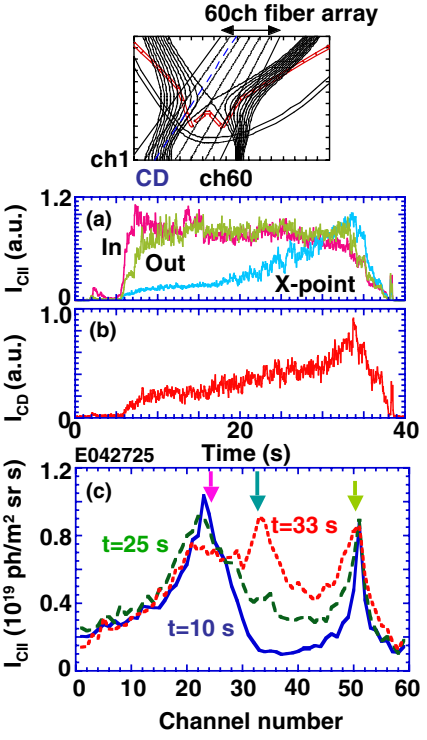

Fig. 6. Time evolution of (a) CII emission intensities measured with the sight lines viewing the inner and outer strike points, and the X-point and (b) CD band emission intensities from the inner divertor in the discharge of E042725. (c) CII emission intensity profiles in the divertor region. Solid, dashed and dotted lines show the data at $t = 10$ s, 25 s and 33 s in the discharge of E042725. The viewing chords are shown in the upper figure. Arrows show the channel number for the sight lines viewing the inner and outer strike points, and the X-point.

around the inner strike point reaches about 500 °C. Since the chemical sputtering yield depends on the surface temperature [12], the change of the temperature of the divertor plates could be related to the change of the CD band emission intensity.

5. Summary

JT-60U research has been expanded to the new area towards steady-state operation by utilizing the long-pulse operation extended to 65 s and the extension of the NB heating pulse length to 30 s. The particle balance analysis in the long-pulse discharge indicates that wall is not saturated even with a high divertor plate temperature around the strike points. However, the wall can be saturated by repeating the several long-pulse discharges. The density increases without gas-puffing in the latter phase of the wall saturated discharge. These results indicate that the absorption area with the low wall temperature is dominant for wall pumping rather than pumping by co-deposited layers. When the wall is saturated, the edge pressure is reduced and the ELMs become close to type III regime. An increase in Dα emission intensity is not observed around the main plasma and in the inner divertor, but is observed upstream of the outer divertor under the wall saturation. The intensities of C II emission near the X-point and CD band emission in the inner divertor start to increase before the wall saturation, and they continue to increase. This could be related to the surface temperature dependence of the chemical sputtering yield.

Acknowledgment

The authors wish to thank the members who have contributed to the JT-60U project especially for modification to the long-pulse operation.

References

[1] ITER Technical Basis, ITER EDA Documentation Series No. 24, IAEA, Vienna, 2002.
[2] S. Nishio et al., Fusion Energy 2000, Sorrento, Italy, 2000, FTP2/14, International Atomic Energy Agency, 2000.
[3] T. Fujita et al., Nucl. Fus. 39 (1999) 1627.
[4] H. Takenaga et al., Nucl. Fus. 41 (2001) 1777.
[5] W. Moller, J. Nucl. Mater. 162–164 (1989) 138.
[6] M. Sakamoto et al., Nucl. Fus. 42 (2002) 165.
[7] J. Jacquinot, Nucl. Fus. 43 (2003) 1583.
[8] F. Saint-Laurent, Nucl. Fus. 40 (2000) 1047.
[9] J. Jacquinot et al., Plasma Phys. Control. Fus. 35 (1993) A35.
[10] Y. Kamada et al., Nucl. Fus. 39 (1999) 1845.
[11] K. Masaki et al., these Proceedings. doi:10.1016/j.jnucmat.2004.10.101.
[12] T. Nakano et al., Nucl. Fus. 42 (2002) 689.